Desalination and Water Treatment
www.deswater.com

doi: 10.5004/dwt.2017.20142

62 (2017) 43–56
February

A shortcut approach to the design of once-through multi-stage flash desalination systems

Mahmoud M. El-Halwagi*

Department of Chemical Engineering, Texas A&M University, College Station, TX 77843, USA, Tel. +1 979 845 3484; Fax: +1 979 845 6446; email: El-Halwagi@tamu.edu

Received 7 May 2016; Accepted 5 August 2016

ABSTRACT

This paper introduces a shortcut method for the design of once-through multi-stage flash systems. The shortcut method is tailored to address the need for conceptual design studies and process synthesis and integration which require compact and computationally efficient models. The use of insightful assumptions leads to the decoupling of the mass balances from the heat balances and from the heat-transfer sizing equations. Such decoupling greatly simplifies the computations and significantly reduces the model size and complexity. Simplified enthalpy correlations are also derived and included in the shortcut method. Comparison with actual plant data shows that the results of the shortcut method compare favorably well with the design and operation data of the existing plant.

Keywords: Design; Process integration; Multi-stage flash; Shortcut

1. Introduction

As a result of the increasing demand for fresh water, desalination technologies continue to receive significant attention. Thermal desalination options include multi-effect evaporation [1,2], multi-stage flash [3,4]. Membrane desalination includes reverse osmosis [5,6], forward osmosis [7,8], and thermal membrane distillation [9,10]. Multi-stage flash (MSF) is a primary desalination approach in which the distillate vapor is generated through flashing. There are two primary configurations for MSF: once-through and brine recirculation. The once-through MSF (OT-MSF) system is schematically shown by Fig. 1. Seawater at its ambient temperature, T_{SW}, enters the system inside tubes that are heated from the outside by condensing distillate vapor. After going through all the effects, the seawater is fed to an evaporator (typically referred to as the brine heater) where external steam is used to further heat the feed so that it reaches its highest temperature within the system ($T_{B,0}$ which is referred to as the top boiling temperature or TBT). Because steam is used as an external utility in this unit, it is referred to as the "heat addition section". The generated distillate vapor exchanges heat with the seawater feed. The result of this heat integration is the condensation of the distillate vapor and the preheating of the seawater feed. Therefore, these effects are collectively called the "heat recovery section." Since the latent heat generated by the condensing distillate is typically higher than the sensible heat gained by the seawater, the flowrate of the incoming seawater is increased by adding flowrate of cooling seawater, CSW, in addition to the flowrate to be desalinated, F, which is subsequently discharged back to the sea. The saturated-liquid brine leaving the first effect enters the second effect through an orifice. The second effect is maintained under a pressure less than that in the first effect. Hence, when the brine from the first effect enters the second effect, it undergoes flashing which leads to the generation of more vapor. The un-flashed saturated-liquid brine leaving the second effect enters the third effect which is maintained at a lower pressure and the flashing process continues. Total flowrate of the collected distillate streams, D, and the final brine stream, B, leave the last effect.

Potential disadvantages associated with OT-MSF include the relatively large flowrate of seawater. Furthermore, the thermal energy contained in the brine is disposed without beneficiation. A possible resolution of these issues is to recycle part

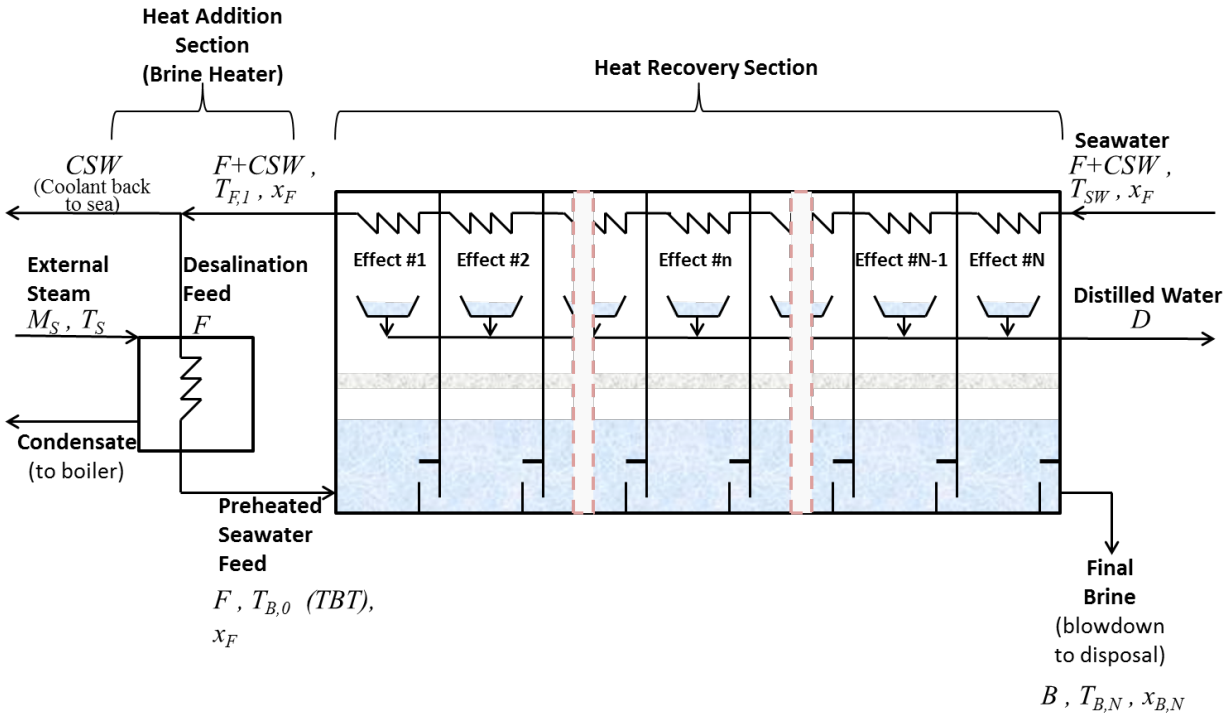

Fig. 1. Representation of OT-MSF.

of the brine and mix it with the feed. This is the basic idea of the brine-recirculation multi-stage flash (BR-MSF) configuration which overcomes the aforementioned disadvantages of OT-MSF through the addition of a brine recycle pump to reduce the flowrate of the raw seawater and a heat rejection section to recover thermal energy from the brine. On the other hand, OT-MSF has several advantages over BR-MSF. These advantages include the simpler design, operation, maintenance, control and the elimination of the capital investment associated with the recirculation pump and the heat rejection section.

Various mathematical models have been developed for OT-MSF. For comprehensive coverage of MSF models, the reader is referred to the literature [1,3,4,11–15]. These detailed models offer valuable tools for estimating the performance of OT-MSF. Nonetheless, there is a critical need for shortcut approaches that can be used in:

- Conceptual design studies that require high-level of a techno-economic studies [16]
- Process synthesis and integration where MSF is coupled with other desalination technologies, heat integration systems, or industrial facilities. Computationally efficient, compact, and simplified models offer distinct advantages in these synthesis and integration studies especially the ones that involve the development of mathematical formulations where the attainment of a global solution is often a challenging task [17–19].

This paper introduces a short-cut approach to the modeling of OT-MSF. The key concept is the decoupling of the mass balance equations from the heat balances and from the heat-transfer sizing equations. The model is particularly suitable for the high-level conceptual design and process synthesis and integration studies.

2. General modeling equations

In this section, the general modeling equations are described for the heat addition and heat recovery sections of the OT-MSF system.

2.1. Modeling the brine heater

Assuming that no evaporation takes place in the brine heater, the latent heat released by the condensing external steam is used to preheat the feed from the temperature of the feed leaving the inside tubes of the first effect ($T_{F,1}$) to the TBT (referred to as $T_{B,0}$). Hence, the enthalpy balance is given by:

$$F[h_F(T_{B,0}) - h_F(T_{F,1})] = M_S \Delta H_{vw,S} \tag{1}$$

The heat transfer area can be calculated from:

$$A_{BH} = \frac{Q_{BH}}{U_{BH} \Delta T_{lm,BH}} \tag{2}$$

with

$$Q_{BH} = M_S \Delta H_{vw,S} \tag{3}$$

And, the logarithmic mean temperature difference is calculated by:

$$\Delta T_{lm,BH} = \frac{T_{B,0} - T_{F,1}}{\ln\left(\frac{T_S - T_{F,1}}{T_S - T_{B,0}}\right)} \tag{4}$$

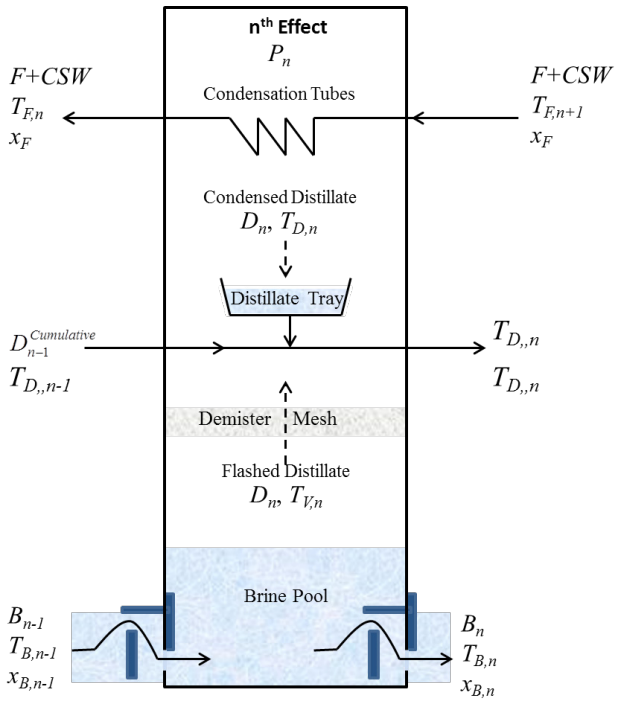

Fig. 2. Representation of the n^{th} Effect of OT-MSF.

2.2. Modeling the MSF Stages

Consider Fig. 2 which shows the nth effect within the heat-recovery section. The following equations describe the key phenomena.

For the flashing brine pool:

Overall mass balance:

$$B_{n-1} = D_n + B_n \qquad n=1,2,\ldots,N \qquad (5)$$

Salt balance (assuming pure distillate):

$$B_{n-1}x_{B,n-1} = B_n x_{B,n} \qquad n=1,2,\ldots,N \qquad (6)$$

Enthalpy balance:

$$B_{n-1}h_{B,n-1} = D_n\Delta H_{vw,D_n} + B_n h_{B,n} \qquad n=1,2,\ldots,N \qquad (7)$$

The brine pool flashes the distillate at a temperature of $T_{V,n}$. Because of the elevation in boiling point, the brine pool temperature is given by:

$$T_{B,n} = T_{V,n} + BPE_n \qquad (8)$$

where BPE_n is the boiling point elevation in the n^{th} effect.

As the distillate passes through the demister mesh, its temperature slightly drops. Furthermore, the temperature of the distillate may not reach equilibrium with the applied pressure, P_n. The demister losses and the non-equilibrium allowance (NEA) cause the distillate temperature to decreases to $T_{D,n}$. For simplicity, the demister heat loss and the NEA will be ignored in the model, i.e.:

$$T_{D,n} \approx T_{V,n} \qquad n=1,2,\ldots,N \qquad (9)$$

For the condensation tubes:

Enthalpy balance:

$$(F+CSW)(h_{F,n} - h_{F,n+1}) = D_n\Delta H_{vw,D_n} + D_n^{\text{Cumulative}}h_{D,n} - D_{n-1}^{\text{Cumulative}}h_{D,n-1} \qquad n=1,2,\ldots,N \qquad (10)$$

where

$$D_n^{\text{Cumulative}} = \sum_1^n D_n \qquad n=1,2,\ldots,N \qquad (11)$$

In the enthalpy balance equation, the last two terms $(D_n^{\text{Cumulative}}h_{D,n} - D_{n-1}^{\text{Cumulative}}h_{D,n-1})$ represent the sensible heat associated with the cumulative distillate. Since $D_n^{\text{Cumulative}}$ is larger than $D_{n-1}^{\text{Cumulative}}$ but $h_{D,n}$ is smaller than $h_{D,n-1}$ and since the latent heat term $(D_n\Delta H_{vw,Dn})$ is typically much larger than the sensible heat term, Eq. (10) may be approximated by:

$$(F+CSW)(h_{F,n} - h_{F,n+1}) = D_n\Delta H_{vw,D_n} \qquad n=1,2,\ldots,N \qquad (12)$$

The heat transfer area for the condensation tubes of the n^{th} effect, $A_{CT,n}$, is calculated through the following expression:

$$A_{CT,n} = \frac{Q_{CT,n}}{U_{CT,n}\Delta T_{lm,CT,n}} \qquad n=1,2,\ldots,N \qquad (13)$$

where $Q_{CT,n}$ is the heat added to the condensation tubes from the condensing distillate, i.e.:

$$Q_{CT,n} = D_n\Delta H_{vw,D_n} \qquad n=1,2,\ldots,N \qquad (14)$$

and

$$\Delta T_{lm,CT,n} = \frac{T_{F,n} - T_{F,n+1}}{\ln\left(\frac{T_{D,n} - T_{F,n+1}}{T_{D,n} - T_{F,n}}\right)} \qquad n=1,2,\ldots,N \qquad (15)$$

For practical reasons, equal-sized heat-transfer areas of the condensation tube bundles are used for all the effects. Therefore,

$$A_{CT,1} = \ldots = A_{CT,n} = \ldots = A_{CT,N} \qquad (16)$$

The overall heat transfer coefficient for the condensation tubes is best determined through experimental data. Otherwise, approximate correlations may be applied for conceptual design purposes. For the condensation tubes, Al-Fulaij et al. [11] proposed the following correlation for the overall heat transfer coefficient, U_{CT}, for the condensation tubes that preheat the seawater/brine feed in the MSF stages:

$$U_{CT} = 0.107309 * (T_V - 273)^{0.773247} * VL^{0.484958} \qquad (17)$$

where U_{CT} is in kW/m^2 K, T_V is in K, and VL (seawater/brine feed velocity inside the tubes) is in m/s.

3. A shortcut approach to the design of OT-MSF

For OT-MSF systems with a large number of stages, the solution of the modelling equations may be laborious.

In this section, a shortcut approach is developed for use in conceptual design and preliminary cost-estimation studies as well as process synthesis and integration applications involving the coupling of MSF with other technologies, heat integration, and industrial processes. The key concept is the decoupling of the mass balance equations from the heat balances and from the heat-transfer sizing equations. The brine heater design is also separated from the design of MSF effects to enable the heater to have a surface area that is not necessarily the same as the flash units and to handle the specific conditions of the external steam.

The flowrate of the distillate is distributed equally over the flash chambers, i.e.:

$$D_n = \frac{D}{N} \qquad n=1,2,\ldots,N \tag{18}$$

The temperatures of the brine and distillate are assumed to be the same (by neglecting the NEA and BPE):

$$T_{V,n} \approx T_{B,n} \qquad n=1,2,\ldots,N \tag{19}$$

In general, the TBT, outlet flashing brine temperature, and preheated feed leaving the first flash chamber are optimization variables. In the shortcut method, these values are fixed by selecting heat-transfer driving forces for the brine heater and for the condensation tubes in the last and the first flash chambers. Therefore,

$$TBT = T_S - \Delta T_1^{\min} \tag{20}$$

where T_S is the temperature of the external steam used in the brine heater and $\Delta T_1^{\min}$ is the selected value of the heat-transfer driving force between steam and the brine leaving the heater.

$$T_{B,N} = T_{SW} + \Delta T_2^{\min} \tag{21}$$

where T_{SW} is the ambient temperature of the seawater entering the last effect and $\Delta T_2^{\min}$ is the selected value of the heat-transfer driving force between the ambient seawater and the brine leaving the last effect.

$$T_{F,1} = TBT - \Delta T_3^{\min} \tag{22}$$

where $T_{F,1}$ is the temperature of the feed leaving the first effect and $\Delta T_3^{\min}$ is the selected value of the heat-transfer driving force between TBT and the feed stream leaving the first effect.

For a large number of flash chambers, it is reasonable to assume that the temperature profile of the flashing brine is linear with respect to the stage number, i.e.:

$$T_{B,n} = T_{B,n-1} - \frac{TBT - T_{B,N}}{N} \tag{23}$$

An average-condition "AC" approach is adopted for calculating the heat transfer area of the condensation tubes. Only one flash effect is modeled to represent the equal-area condensation tubes for all the flash chambers. The average distillate temperature is defined as:

$$T_{V,avg} \approx \frac{TBT + T_{B,N}}{2} \tag{24}$$

and the total heat duty of all the condensation tubes is given by:

$$Q_{CT,\text{Total}} = \Delta H_{vw,avg} D \tag{25}$$

with the latent heat of condensation calculated by the correlation obtained in Appendix I:

$$\Delta H_{vw,avg} = -2.7532 t_{V,avg} + 3278.8 \tag{26}$$

The heat transfer area of the condensation tubes in the AC flash chamber, $A_{CT,AC}$, may be determined from:

$$Q_{CT,AC} = U_{CT,AC} A_{CT,AC} \Delta T_{AC} \tag{27}$$

where

$$Q_{CT,AC} = \frac{Q_{CT,\text{Total}}}{N} \tag{28}$$

$$\Delta T_{AC} = T_{V,avg} - T_{F,avg} \tag{29}$$

$$T_{F,avg} = \frac{T_{SW} + T_{F,1}}{2} \tag{30}$$

The overall heat transfer coefficient, $U_{CT,AC}$, is calculated at the average temperature of the distillate.

Since all effects are designed to have equal heat transfer areas of the condensation tubes, then the total area of the condensation tubes if determined through:

$$A_{CT}^{\text{Total}} = N * A_{CT,AC} \tag{31}$$

The flowrate of the cooling seawater may be calculated from enthalpy balance:

$$(F + CSW) * c_{p,SW} * (T_{F,1} - T_{SW}) = Q_{CT,\text{Total}} \tag{32}$$

4. Case study: using the shortcut method to design an OT-MSF system

Al-Fulaij et al. [11] reported the data of an existing 21-stage OT-MSF plant. The feed flowrate to be desalinated is 4,027 kg/s and it has a salinity of 40‰. The plant produces 378 kg/s of desalinated water with almost no salts in it. The following data are available:

- T_S = 384 K
- TBT = 364 K (i.e., $\Delta T_1^{\min}$ = 20 K)
- T_{SW} = 310.7 K
- $T_{B,N}$ = 315.7 K (i.e., $\Delta T_2^{\min}$ = 5 K)
- $T_{F,1}$ = 334 K (i.e., $\Delta T_3^{\min}$ = 30 K)

The condensation tubes have a length of 3.15 m per chamber and an outside diameter of 0.0445 m.

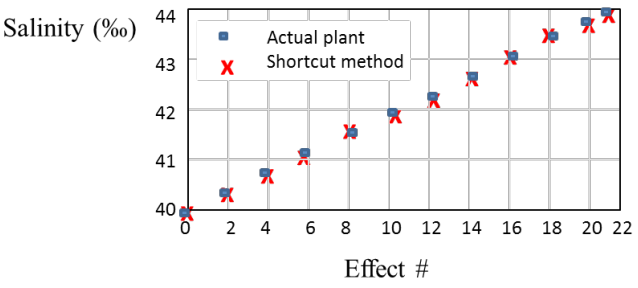

Fig. 3. Comparison of the theoretical prediction of flashing brine salinity with actual plant data.

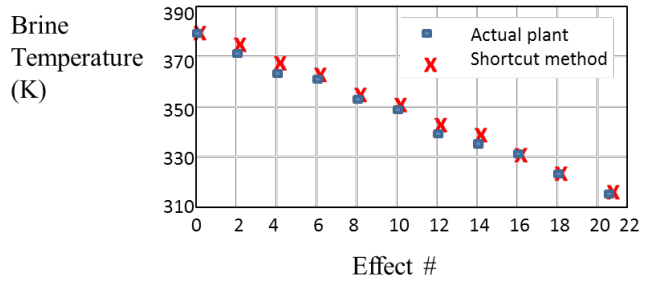

Fig. 4. Comparison of the theoretical prediction of flashing brine temperature with actual plant data.

The shortcut method may be solved through hand calculations. For convenience and potential coupling with optimization studies (e.g., process synthesis and integration), the mathematical code is given in the supplementary materials at the end of this paper. The solution of the shortcut method matches the distillate flowrate and predicts the need to use 1,427 condensation tubes. The actual plant uses 1,410 tubes. Figs. 3 and 4 compare the results of the shortcut method with the actual plant data reported by Al-Fulaij et al. [11]. As can be seen from the figures, there is results of the shortcut methods compare favorably well with the actual plant data.

5. Conclusions

A shortcut method has been presented for the design of OT-MSF systems. By decoupling the computations associated with the mass balances, heat balances, and sizing of the heat-transfer areas, the model size and complexity are significantly reduced rendering it attractive for conceptual design and process synthesis and integration applications. Simplified enthalpy correlations have also been derived and included in the shortcut method. A case study involving data from an actual OT-MSF plant was used to assess the validity of the proposed shortcut method. The results of the shortcut method and the data from the existing plant are in excellent agreement.

Symbols

A — Heat transfer area, m^2
B — Brine flowrate, kg/s
BPE — Boiling point elevation, K
$c_{p,SW}$ — Specific heat of seawater, kJ/kg K
CSW — Flowrate of cooling water, kg/s
D — Distillate flowrate, kg/s
F — Feed flowrate, kg/s
h — Specific enthalpy of liquid, kJ/kg
H — Specific enthalpy of vapor
M_S — Flowrate of steam; kg/s
n — Effect number
N — Total number of effects
Q — Rate of heat transfer, kW
T — Temperature, K
TBT — Top boiling temperature, K
U — Overall heat transfer coefficient, kW/m^2 K
VL — Seawater/brine feed velocity inside the tubes, m/s
x — Mass fraction

Greek

ΔH_{vw} — Latent heat of condensation, kJ/kg
ΔT_{AC} — Difference between average vapor temperature and average feed temperature, K
ΔT_{lm} — Logarithmic mean temperature difference, K
$\Delta T^{\min}$ — Heat-transfer driving force, K

Subscripts

avg — Average
B — Brine
CT — Condensing tubes
D — Distillate
F — Feed
n — Effect number
N — Total number of effects
S — Steam
SW — Seawater
V — Vapor

References

[1] H. El-Dessouky, H. Ettouney, Fundamentals of Salt Water Desalination, Elsevier, Amsterdam, 2002.
[2] I.S. Al-Mutaz, Features of multi-effect evaporation desalination plants, Desal. Wat. Treat., 54 (2014) 3227–3235.
[3] H.T. El-Dessouky, I. Alatiqi, H.M. Ettouney, Process synthesis: the multistage flash desalination system, Desalination, 115 (1998) 155–179.
[4] M.M.A. Raja, K.K. Murugavela, T. Rajaseenivasanb, K. Sritharb, A review on flash evaporation desalination, Desal. Wat. Treat., 57 (2016) 13462–13471.
[5] C.S. Khor, D.C.Y. Foo, M.M. El-Halwagi, R.R. Tan, N. Shah, A superstructure optimization approach for membrane separation-based water regeneration network synthesis with detailed nonlinear mechanistic reverse osmosis model, Ind. Eng. Chem. Res., 50 (2011) 13444–13456.
[6] M.M. El-Halwagi, Synthesis of optimal reverse-osmosis networks for waste reduction, AIChE J., 38 (1992) 1185–1198.
[7] M.T.M. Pendergast, M.S. Nowosielski-Slepowron, J. Tracy, Going big with forward osmosis, Desal. Wat. Treat., 57 (2016) 26529–26538.
[8] T.Y. Cath, A.E. Childress, M. Elimelech, Forward osmosis: principles, applications, and recent developments, J. Membr. Sci., 281 (2006) 70–87.
[9] R. González-Bravo, F. Nápoles-Rivera, J.M. Ponce-Ortega, M. Nyapathi, N.A. Elsayed, M.M. El-Halwagi, Synthesis of optimal thermal membrane distillation networks, AIChE J., 61 (2015) 448–463.

[10] N.A. Elsayed, M.A. Barrufet, M.M. El-Halwagi, Integration of thermal membrane distillation networks with processing facilities, Ind. Eng. Chem. Res., 53 (2014) 5284–5298.
[11] H. Al-Fulaij, A. Cipollina, D. Bogle, H. Ettouney, Once through multistage flash desalination: gPROMS dynamic and steady state modeling, Desal. Wat. Treat., 18 (2010) 46–60.
[12] M.B. Ali, L. Kairouani, Solving equations describing the steady-state model of msf desalination process using solver optimization tool of Matlab software, Desal. Wat. Treat., 52 (2014) 7473–7483.
[13] J. Gebel, Thermal Desalination Processes, Desalination: Water from Water, Ed. J. Kucera, Scrivener Pub., Beverly, MA, USA, 2014, pp. 41–154.
[14] M. Rosso, A. Beltmmini, M. Mazzotti, M. Morbidelli, Modeling multistage flash desalination plants, Desalination, 108 (1996) 365–374.
[15] M.S. Tanvir, I.M. Mujtaba, Optimisation of design and operation of msf desalination process using MINLP technique in gPROMS, Desalination, 222 (2008) 419–430.
[16] M.M. El-Halwagi, Sustainable Design through Process Integration: Fundamentals and Applications to Industrial Pollution Prevention, Resource Conservation, and Profitability Enhancement, Butterworth-Heinemann/Elsevier, Oxford, UK, 2012.
[17] K. Gabriel, M.M. El-Halwagi, P. Linke, Optimization across water-energy nexus for integrating heat, power, and water for industrial processes coupled with hybrid thermal-membrane desalination, Ind. Eng. Chem. Res., 55 (2016) 3442–3466.
[18] K.J. Gabriel, M.M.B. Noureldin, P. Linke, M.M. El-Halwagi, Optimization of multi-effect distillation process using a linear enthalpy model, Desalination, 365 (2015) 261–276.
[19] S. Atilhan, A. Bin-Mahfouz, B. Batchelor, P. Linke, A. Abdel-Wahab, F. Nápoles-Rivera, A. Jiménez-Gutiérrez, M.M. El-Halwagi, A systems-integration approach to the optimization of macroscopic water desalination and distribution networks: a general framework applied to qatar's water resources, Clean Technol. Environ. Policy, 14 (2012) 161–171.
[20] C.F. Beaton, G.F. Hewitt, Physical Property Data for the Chemical and Mechanical Engineer, Hemisphere Publishing Corp., Taylor and Francis, New York, 1989.
[21] M.H. Sharqawy, J.H. Lienhard, S.M. Zubair, Thermophysical properties of seawater: a review of existing correlations and data, Desal. Wat. Treat., 16 (2010) 354–380.
[22] L.A. Bromley, Relative enthalpies of sea salt solutions at 25°C, J. Chem. Eng. Data, 13 (1968) 399–402.
[23] D.N. Connors, On the enthalpy of seawater, Limnol. Oceanography, 15 (1970) 587–594.
[24] L. Schrage, Optimization Modeling with LINGO, 6th ed., LINDO Systems, Chicago, 2006.

Appendix I

I. Shortcut correlations for enthaply calculations

I.1. Pure water enthalpy

Before addressing the enthalpy and specific heat capacity (or specific heat for short) of seawater, it is beneficial to first consider these properties for pure water. The enthalpy and specific heat of pure water may be obtained from experimental data given in the steam tables. For regression purposes, enthalpy data for pure water from steam tables under saturation conditions (e.g., [20]) were considered over the temperature range of 273–443 K and the corresponding saturation pressure. The used data included the specific enthalpy of saturated water, h_w, saturated vapor, H_v, and latent heat of vaporization, ΔH_{vw} (which is equal to $H_v - h_w$ Linear regression of these data is used to develop the following approximate correlations:

$$h_w = 4.2288T - 1156.8 \qquad R^2 = 0.9999 \text{ for } 293 \le T\,(K) \le 443 \tag{I.1}$$

$$\Delta H_{vw} = -2.7532T + 3278.8 \qquad R^2 = 0.9976 \text{ for } 323 \le T\,(K) \le 443 \tag{I.2}$$

where h_w is in kJ/kg and T is the saturation temperature in K. The enthalpy of water vapor may be calculated as:

$$H_v = h_w + \Delta H_{vw} \tag{I.3}$$

I.2. Seawater enthalpy

The enthalpy of seawater, h_{sw}, may be calculated from the enthalpy of pure water, salinity, and temperature. Sharqawy et al. [21] proposed the following expression:

$$h_{sw} = h_w - 0.001x_s(a_1 + a_2x_s + a_3x_s^2 + a_4x_s^3 + a_5\,(\text{T-273}) + a_6(\text{T-273})^2$$

$$+ a_7\,(\text{T-273})^3 + a_8x_s(\text{T-273}) + a_9x_s^2(\text{T-273}) + a_{10}x_s\,(\text{T-273})^2)$$

$$284 \le T \le 393 \text{ K} \qquad 0 \le x_S \le 0.12 \text{ kg/kg} \tag{I.4a}$$

where h_{sw} and h_w (in kJ/kg) are calculated at the same temperature T (in K) with the same reference state (e.g., zero enthalpy at zero K temperature). The mass fraction of the salts, x_s, is related to salinity as follows:

$$x_s\,(\text{kg/kg}) = 0.001\ S‰ \tag{I.4b}$$

The values of the coefficients are:

$$a_1 = -2.348*10^4,\ a_2 = 3.152*10^5,\ a_3 = 2.803*10^6,\ a_4 = -1.446*10^7,$$
$$a_5 = 7.826*10^3,\ a_6 = -4.417*10^1,\ a_7 = 2.139*10^{-1},\ a_8 = -1.991*10^4,$$
$$a_9 = 2.778*10^4,\ a_{10} = 9.728*10^1 \tag{I.4c}$$

The accuracy of Eq. (I.4) is ±0.5% from the data reported by the International Association for the Properties of Water and Steam (IAPWS, 2008 which may be downloaded from http://www.iapws.org/relguide/Seawater.html). For conceptual design and optimization purposes, it is useful to consider simpler forms of the enthalpy correlation. Based on the experimental data of Bromley [22], Connors [23] observed that while near-infinite dilution of seawater, the enthalpy changes approximately as the square root of salinity, it shows a rather linear dependence on salinity in the range of 10‰ to 70‰. Let us examine the possibility of developing a form which is simpler than Eq. (I.4). Suppose that:

$$h_{sw} = h_w + aS \tag{I.5}$$

where a is function of temperature. First, Eq. (I.1) is used to estimate the enthalpy of pure liquid water at different temperatures. Through statistical analysis of the data for seawater enthalpy in conjunction with the proposed form of Eq. (I.5), the following correlation is obtained:

$$h_{sw} = h_w - (0.0048T - 1.2702)S \tag{I.6}$$

Over the following ranges:

$$293 \le T\,(K) \le 373 \text{ and } 10 \le S‰ \le 100$$

with h_{sw} and h_w (in kJ/kg) to be calculated at the same temperature T (in K) with the same reference state. The value of h_w may be obtained from the steam tables of from correlations such as Eq. (I.1).

Table I.2 shows a comparison between the predictions of Eqs. (I.4) and (I.6). The simplified Eq. (I.6) performs reasonably well compared to Eq. (I.4). For conceptual and optimization studies, Eq. (I.6) has the advantage of the much simpler mathematical form.

Table I.2.
Comparison of the Simplified Correlation (Eq. I.6) with the Detailed Correlation (Eq. I.4) for Estimating the Enthalpy of Seawater, h_{sw} in kJ/kg, at Different Temperatures and Salinities

T	S = 10‰	S=10‰	S= 35‰	S =35‰	S = 60‰	S = 60‰	S = 100‰	S =100‰
K	Eq. (35)	Eq. (38)	Eq. (35)	Eq. (38)	Eq. (35)	Eq. (38)	Eq. (35)	Eq. (38)
293	82.7	82.4	79.7	79.0	76.5	75.6	70.7	70.2
313	165.2	165.2	159.6	159.4	154.1	153.6	145.0	144.2
333	247.8	247.8	239.9	239.6	232.2	231.4	220.0	218.3
353	330.6	330.6	320.4	320.0	310.5	309.3	284.8	292.4
373	413.6	413.7	400.9	400.7	388.5	387.7	368.6	366.9

Supplementary materials
mathematical programming code for the shortcut method

LINGO® is a software that solves linear, nonlinear and mixed integer linear and nonlinear programs. Information on the software can be obtained from LINGO® User's Guide [24]. The following program is the formulation of the shortcut method coded in LINGO® for the case study.

```
SETS:

SET_EFFECTS/1..22/:B, xB, LambdaD, TF, Tv, TB;

ENDSETS


Total_Distillate = 378;

Neffects = 21;

D = Total_Distillate/Neffects;

F = 4027;

F = B(1);

xF = 0.04;

xF = xB(1);


TBT = TS - DeltaT1;

TBT = TB(1);

TS = 384;

DeltaT1 = 20;

TF_Raw = 310.7;

TB_out = TF_Raw + DeltaT2;

TF_Raw = 310.7;

DeltaT2 = 5;

TF(1) = TBT - DeltaT3;

DeltaT3 = 30;

TF_Raw = 310.7;

hF_Raw = 4.2288*TF_Raw - 1156.8 - (0.0048*TF_Raw - 1.2702)*xF*1000;

DTB = (TBT - TB_out)/Neffects;

TV_Avg = (TBT + TB_out)/2;

LambdaD_Avg = -2.7532*TV_Avg + 3278.8;

UCT_Avg = 0.0454*TV_Avg -11.586;
```

```
@FOR(SET_EFFECTS(n)| n#GE# 2:

TB(n) = TB(n-1) - DTB;

TV(n) = TB(n);

LambdaD(n) = -2.7532*TV(n) + 3278.8;

B(n-1) = D + B(n);

B(n-1)*xB(n-1) = B(n)*xB(n));

QCT = @SUM(Set_Effects(n) |n #GE# 2: D*LambdaD(n));

QCT = (F+CSW)*(hF_1 - hF_Raw);

hF_1 = 4.2288*TF(1) - 1156.8 - (0.0048*TF(1) - 1.2702)*xF*1000;

DTF_Effect = (TF(1) - TF_Raw)/Neffects;

@FOR(SET_EFFECTS(n)| n#GE# 2: TF(n) = TF(n-1) - DTF_Effect);

TF_Avg = (TF(1)+TF_Raw)/2;

QCT = Neffects*UCT_Avg*A*(TV_avg- TF_Avg);

Total_Area = Neffects*A;

OD_tube = 0.0445;

L_tube = 3.15;

A_tube = 3.14*OD_tube*L_tube;

N_tubes = A/A_tube;
```

The solution is shown below.

Variable	Value
TOTAL_DISTILLATE	378.0000
NEFFECTS	21.00000
D	18.00000
F	4027.000
XF	0.4000000E-01
TBT	364.0000
TS	384.0000
DELTAT1	20.00000
TF_RAW	310.7000
TB_OUT	315.7000
DELTAT2	5.000000

DELTAT3	30.00000
HF_RAW	148.2418
DTB	2.300000
TV_AVG	339.8500
LAMBDAD_AVG	2343.125
UCT_AVG	3.843190
QCT	886898.1
CSW	5402.324
HF_1	242.2992
DTF_EFFECT	1.109524
TF_AVG	322.3500
A	627.9492
TOTAL_AREA	13186.93
OD_TUBE	0.4450000E-01
L_TUBE	3.150000
A_TUBE	0.4401495
N_TUBES	1426.673
B(1)	4027.000
B(2)	4009.000
B(3)	3991.000
B(4)	3973.000
B(5)	3955.000
B(6)	3937.000
B(7)	3919.000
B(8)	3901.000
B(9)	3883.000
B(10)	3865.000
B(11)	3847.000
B(12)	3829.000
B(13)	3811.000
B(14)	3793.000
B(15)	3775.000
B(16)	3757.000

```
B( 17)        3739.000
B( 18)        3721.000
B( 19)        3703.000
B( 20)        3685.000
B( 21)        3667.000
B( 22)        3649.000
XB( 1)       0.4000000E-01
XB( 2)       0.4017960E-01
XB( 3)       0.4036081E-01
XB( 4)       0.4054367E-01
XB( 5)       0.4072819E-01
XB( 6)       0.4091440E-01
XB( 7)       0.4110232E-01
XB( 8)       0.4129198E-01
XB( 9)       0.4148339E-01
XB( 10)      0.4167658E-01
XB( 11)      0.4187159E-01
XB( 12)      0.4206843E-01
XB( 13)      0.4226712E-01
XB( 14)      0.4246770E-01
XB( 15)      0.4267020E-01
XB( 16)      0.4287463E-01
XB( 17)      0.4308104E-01
XB( 18)      0.4328944E-01
XB( 19)      0.4349986E-01
XB( 20)      0.4371235E-01
XB( 21)      0.4392692E-01
XB( 22)      0.4414360E-01
LAMBDAD( 1)        0.000000
LAMBDAD( 2)        2282.968
LAMBDAD( 3)        2289.300
LAMBDAD( 4)        2295.632
LAMBDAD( 5)        2301.965
```

LAMBDAD(6)	2308.297
LAMBDAD(7)	2314.629
LAMBDAD(8)	2320.962
LAMBDAD(9)	2327.294
LAMBDAD(10)	2333.626
LAMBDAD(11)	2339.959
LAMBDAD(12)	2346.291
LAMBDAD(13)	2352.624
LAMBDAD(14)	2358.956
LAMBDAD(15)	2365.288
LAMBDAD(16)	2371.621
LAMBDAD(17)	2377.953
LAMBDAD(18)	2384.285
LAMBDAD(19)	2390.618
LAMBDAD(20)	2396.950
LAMBDAD(21)	2403.282
LAMBDAD(22)	2409.615
TF(1)	334.0000
TF(2)	332.8905
TF(3)	331.7810
TF(4)	330.6714
TF(5)	329.5619
TF(6)	328.4524
TF(7)	327.3429
TF(8)	326.2333
TF(9)	325.1238
TF(10)	324.0143
TF(11)	322.9048
TF(12)	321.7952
TF(13)	320.6857
TF(14)	319.5762
TF(15)	318.4667
TF(16)	317.3571

TF(17)	316.2476
TF(18)	315.1381
TF(19)	314.0286
TF(20)	312.9190
TF(21)	311.8095
TF(22)	310.7000
TV(1)	0.000000
TV(2)	361.7000
TV(3)	359.4000
TV(4)	357.1000
TV(5)	354.8000
TV(6)	352.5000
TV(7)	350.2000
TV(8)	347.9000
TV(9)	345.6000
TV(10)	343.3000
TV(11)	341.0000
TV(12)	338.7000
TV(13)	336.4000
TV(14)	334.1000
TV(15)	331.8000
TV(16)	329.5000
TV(17)	327.2000
TV(18)	324.9000
TV(19)	322.6000
TV(20)	320.3000
TV(21)	318.0000
TV(22)	315.7000
TB(1)	364.0000
TB(2)	361.7000
TB(3)	359.4000
TB(4)	357.1000
TB(5)	354.8000

TB(6)	352.5000
TB(7)	350.2000
TB(8)	347.9000
TB(9)	345.6000
TB(10)	343.3000
TB(11)	341.0000
TB(12)	338.7000
TB(13)	336.4000
TB(14)	334.1000
TB(15)	331.8000
TB(16)	329.5000
TB(17)	327.2000
TB(18)	324.9000
TB(19)	322.6000
TB(20)	320.3000
TB(21)	318.0000
TB(22)	315.7000